APPROXIMATE DECONVOLUTION AND EXPLICIT FILTERING FOR LES OF A PREMIXED TURBULENT JET-FLAME

P. Domingo and L. Vervisch

[1] *CORIA-CNRS & Normandie Université, INSA de Rouen, France*

domingo@coria.fr

1 Introduction

The modeling strategies for Large Eddy Simulation (LES) of premixed flames have been based mainly on G-Eq (Peters 2000; Moureau et al. 2009), flame surface density (Hawkes and Cant 2001; Lecocq et al. 2011) and laminar flamelets combined with various forms of presumed probability density function (pdf) to express flame filtering (Kim et al. 1999; Domingo et al. 2005; Fiorina et al. 2010; Moureau et al. 2011; Lecocq et al. 2011; Nambully et al. 2014a; Nambully et al. 2014b). Artificial thickening of the flame front (Colin et al. 2000; Kuenne et al. 2012; Boudier et al. 2008) is another successful alternative.

A fully new modeling strategy is discussed in this paper, in which an approximate deconvolution is combined with explicit filtering to express the sub-grid scale (SGS) terms of scalar fields.

This idea goes back to the fundamentals of LES grounded on physical space filtering, instead of introducing an ad-hoc treatment of the phenomena which are unresolved by the grid.

The proposed method, called ADEF (Approximate Deconvolution and Explicit flame Filtering), may be applied to any form of chemical description, Arrhenius expressions or tabulated chemistry.

First, the method is applied to a canonical laminar one-dimensional filtered flame. Then, LES of a three-dimensional turbulent premixed jet flame is performed and results are compared against measurements by Chen et al. (1996).

2 ADEF Modeling

Approximate deconvolution

A Taylor expansion is written for the scalar field in every 'j' direction:

$$\begin{aligned}\varphi(x'_j,t) &= \varphi(x_j,t) + (x'_k - x_k)\frac{\partial\varphi(x_j,t)}{\partial x_k} \qquad (1)\\ &+ \frac{1}{2}(x'_k - x_k)(x'_\ell - x_\ell)\frac{\partial^2\varphi(x_j,t)}{\partial x_k \partial x_\ell} + \cdots\end{aligned}$$

Repeated indices implies a sommation over the three directions. A Gaussian filter is applied to relation (1), all terms with odd power of the position are eliminated due to the filter symmetry. For turbulent scalar signals, the fourth order terms were not found to play a major role, and the filtering may be achieved with only the second order derivatives (Katopodes et al. 2000):

$$\overline{\varphi}(\underline{x},t) = \varphi(\underline{x},t) + \frac{\Delta^2}{24}\frac{\partial^2\varphi}{\partial x_i \partial x_i} + \mathcal{O}(\Delta^4)\,. \qquad (2)$$

The relation (2) may be used recursively, and rearranging leads to an approximate and discrete deconvolution operation :

$$\varphi(\underline{x},t) = \mathcal{L}_\Delta^{-1}[\overline{\varphi}(\underline{x},t)] = \overline{\varphi}(\underline{x},t) - \frac{\Delta^2}{24}\frac{\partial^2\overline{\varphi}}{\partial x_i \partial x_i}\,. \qquad (3)$$

A density weighted scalar deconvolution may also be introduced as:

$$\begin{aligned}\varphi(\underline{x},t) &= \frac{\mathcal{L}_\Delta^{-1}[\overline{\rho(\underline{x},t)\varphi(\underline{x},t)}]}{\mathcal{L}_\Delta^{-1}[\overline{\rho}(\underline{x},t)]} \qquad (4)\\ &= \frac{\mathcal{L}_\Delta^{-1}[\overline{\rho}(\underline{x},t)\widetilde{\varphi}(\underline{x},t)]}{\mathcal{L}_\Delta^{-1}[\overline{\rho}(\underline{x},t)]}\\ &= \widetilde{\mathcal{L}}_\Delta^{-1}[\widetilde{\varphi}(\underline{x},t)]\,. \qquad (5)\end{aligned}$$

The relations (2) and (3) may be used in explicit or implicit numerical formulations.

Application to flames

Filtering the φ-balance equation of a scalar used to describe a flame front leads to:

$$\begin{aligned}\frac{\partial\overline{\rho}\widetilde{\varphi}}{\partial t} + \nabla\cdot(\overline{\rho}\widetilde{\mathbf{u}}\widetilde{\varphi}) &= \nabla\cdot\left(\overline{\rho}D_\varphi(\underline{\widetilde{\varphi}})\nabla\widetilde{\varphi}\right) + \overline{\dot{\omega}}_\varphi\\ &- \nabla\cdot\left(\tau_{u_\varphi} - \tau_{D_\varphi}\right)\,, \qquad (6)\end{aligned}$$

where usual notations are adopted. The filtered burning rate $\overline{\dot{\omega}}_\varphi$ plus two unresolved flux terms appear:

$$\tau_{u_\varphi} = \overline{\rho\mathbf{u}\varphi} - \overline{\rho}\,\widetilde{\mathbf{u}}\,\widetilde{\varphi}\,, \qquad (7)$$

$$\tau_{D_\varphi} = \overline{\rho D_\varphi \nabla\varphi} - \overline{\rho}D_\varphi(\widetilde{\varphi})\nabla\widetilde{\varphi}\,. \qquad (8)$$

To perform LES, τ_{u_φ} and τ_{D_φ} must be expressed from quantities resolved over the coarse mesh. Similarly, because of the non-linear character of chemistry $\overline{\dot{\omega}}_\varphi \neq$

$\dot{\omega}_\varphi(\widetilde{\varphi})$, and a specific strategy must be developed to express the filtered chemical source.

All these terms may be computed from deconvolution operations providing approximations of unfiltered values, used to compute terms in their primitive form before they are filtered. In other words, Eq. (5) is applied to get an approximation of $\varphi(\underline{x},t)$, this approximation is used to compute unresolved terms, which are subsequently filtered using Eq. (2).

For instance, the chemical source may be estimated with the mass fractions and temperature obtained with deconvolution, to be then explicitly filtered:

$$\overline{\dot{\omega}}_\varphi(\underline{x},t) = \overline{\dot{\omega}_\varphi(\widetilde{\mathcal{L}}_\Delta^{-1}[\widetilde{\underline{\varphi}}(\underline{x},t)])}\,. \tag{9}$$

In practice, $\widetilde{\varphi}(\underline{x},t)$ is resolved by the LES mesh, but the signal $\dot{\omega}_\varphi(\widetilde{\mathcal{L}}_\Delta^{-1}[\widetilde{\underline{\varphi}}(\underline{x},t)])$ may not be fully resolved by this mesh and a specific numerical treatment needed.

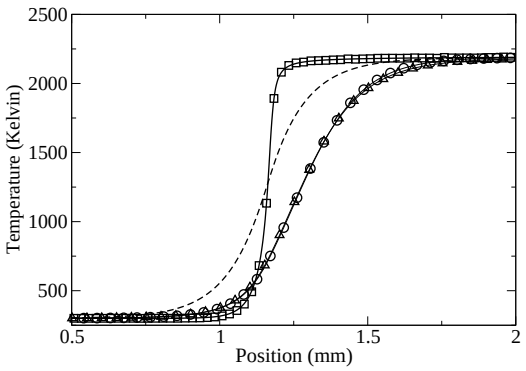

Figure 1: Temperature profiles. From Eq. (10) Line: $T(x)$; Dash-line: $\overline{T}(x)$; Line with circle: $\widetilde{T}(x)$. From solving Eq. (15); Line with triangle: $\widetilde{T}(x)$. Square: $T(x)$ from deconvolution. $\Delta/\delta_{fl} = 8$.

3 Canonical one-dimensional filtered flame with Arrhenius reaction rate

Before assessing the prediction capabilities of approximate deconvolution in a three-dimensional turbulent flame with tabulated detailed chemistry, it is verified that simulating a planar and steady filtered flame preserves the flame major properties, as flame speed and flame thickness, but also profiles filtered across the flame for various filter sizes. A single-step Arrhenius chemistry is considered, to test the possibility of directly solving for chemistry, *i.e.* avoiding chemistry tabulation in future LES of 3D flows.

The one-dimensional canonical problem is cast in terms of the temperature equation:

$$\frac{\partial \rho T}{\partial t} + \nabla\cdot\,(\rho \mathbf{u} T) = \nabla\cdot(a_T(T)\nabla T) + \dot{\omega}_T\,, \tag{10}$$

with

$$\dot{\omega}_T = K_o(T_b - T_o)\rho Y_F Y_O^2 \exp\left(-\frac{T_{Ac}}{T}\right)\,, \tag{11}$$

where $K_o = 170\cdot 10^{12}$ s^{-1}, $Y_F = Z_s Y_{F,o}(1-c)$, $Y_O = (1-Z_s)Y_{O,o}(1-c)$ with $c = (T-T_o)/(T_b - T_o)$, $Z_s = 0.055$, $Y_{F,o} = 1$, $Y_{O,o} = 0.23$ and $T_{Ac} = 19105$ K. The Sutherland law for the diffusion coefficient response versus temperature is introduced: $a_T = a_{T_o}(1+C_s/T_s)/(1+C_s/T)\sqrt{(T/T_s)}$ with $a_{T_o} = 2.086\cdot 10^{-5}$ m$^2\cdot$s^{-1}, $C_s = 120$ and $T_s = 291.15$ K. The fresh and burnt gases temperatures are taken as: $T_o = 300$ K and $T_b = 2200$ K, respectively. The one-dimensional unstrained flame then propagates at $S_L = 0.47$ m$\cdot$s^{-1}; hence for this preliminary test, the parameters have been chosen to produce a laminar flame representative of simple hydrocarbon burning in oxidizer, under the stoichiometric condition.

Approximate deconvolution/filtering for fluxes and sources

Assuming constant pressure and molar mass, the filtered density only depends on the filtered temperature $\overline{\rho T} = \overline{\rho}\widetilde{T} = \rho_o T_o$. The mass conservation reads $\rho_o S_L = \overline{\rho u} = \overline{\rho}\,\widetilde{u}$, and the velocity $\widetilde{u} = (\widetilde{T}/T_o)S_L$ is also a function of $\widetilde{T}$. The SGS convective term becomes for this simple planar flame:

$$\begin{aligned}
\tau_{u_T} &= \overline{\rho \mathbf{u} T} - \overline{\rho}\,\widetilde{\mathbf{u}}\,\widetilde{T}\,, &(12)\\
&= \rho_o S_L(\overline{T} - \widetilde{T})\,, &(13)\\
&= \rho_o S_L\left(\overline{\widetilde{\mathcal{L}}_\Delta^{-1}[\widetilde{T}]} - \widetilde{T}\right)\,. &(14)
\end{aligned}$$

Similarly, the SGS diffusive term τ_{D_T} is obtained from deconvolution and explicit filtering, leading to the closed form of Eq. (6) for the temperature:

$$\begin{aligned}
&\frac{\partial \widetilde{T}}{\partial t} + \underbrace{\widetilde{u}\cdot\nabla\widetilde{T}}_{\text{(i)}} = \underbrace{\frac{1}{\overline{\rho}}\nabla\cdot\left(\overline{\rho}a_T(\widetilde{T})\nabla\widetilde{T}\right)}_{\text{(ii)}} + \underbrace{\frac{\overline{\dot{\omega}_T(\widetilde{\mathcal{L}}_\Delta^{-1}[\widetilde{T}])}}{\overline{\rho}}}_{\text{(iii)}}\\
&\underbrace{-\frac{\rho_o}{\overline{\rho}}S_L\nabla\left(\overline{\widetilde{\mathcal{L}}_\Delta^{-1}[\widetilde{T}]} - \widetilde{T}\right)}_{\text{(iv)}} \qquad (15)\\
&+\underbrace{\frac{1}{\overline{\rho}}\nabla\cdot\left(\overline{\rho(\widetilde{\mathcal{L}}_\Delta^{-1}[\widetilde{T}])a_T(\widetilde{\mathcal{L}}_\Delta^{-1}[\widetilde{T}])\nabla\widetilde{\mathcal{L}}_\Delta^{-1}[\widetilde{T}]} - \overline{\rho}a_T(\widetilde{T})\nabla\widetilde{T}\right)}_{\text{(v)}}\,.
\end{aligned}$$

To check the validity of approximate deconvolution/explicit filtering in this canonical case, the following procedure is applied. (I): the primitive equation (10) is solved with a sixth order PADE scheme (Lele 1992) for spatial discretization and third order compact Runge-Kutta for time-stepping. This provides a

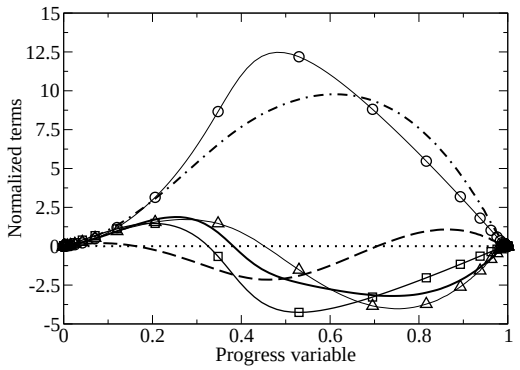

(a) $\Delta/\delta_{\mathfrak{fl}} = 3$.

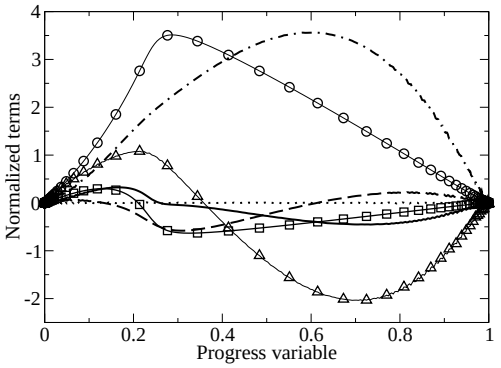

(b) $\Delta/\delta_{\mathfrak{fl}} = 8$.

Figure 2: Terms of Eq. (15) *vs* filtered progress variable. Dash-dot: Resolved convection (i). Line: Resolved diffusion (ii). Circle: Chemical source (iii). Triangle: SGS convection (iv). Dash: SGS molecular diffusion (v). Square: Total molecular diffusion $(ii) + (v)$. Dotted: budget. Quantities are normalized by $(S_L T_o)/\delta_{\mathfrak{fl}}$.

reference laminar flame with a high-resolution $h = \delta_{fl}/30$, where δ_{fl} is the thermal flame thickness. (II): the modeled Eq. (15) is solved with the same numerical methods, but with a mesh spacing $h = \Delta/2$, where Δ is the filter size. A second order interpolation is then added between the coarse mesh points when computing and filtering the chemical source from deconvoluted temperature. (III): the solution of (II) is compared against the reference solution of (I) Gaussian filtered at Δ.

The deconvolution procedure followed by explicit filtering applied in Eq. (15) exactly reproduces the Gaussian filtered flame, as seen in Fig. 1 (without any sub-model, the flame cannot be converged over the coarse mesh). Tests were performed for a range of filters with similar agreement. In these simulations, the flame speed computed from the integral of the burning

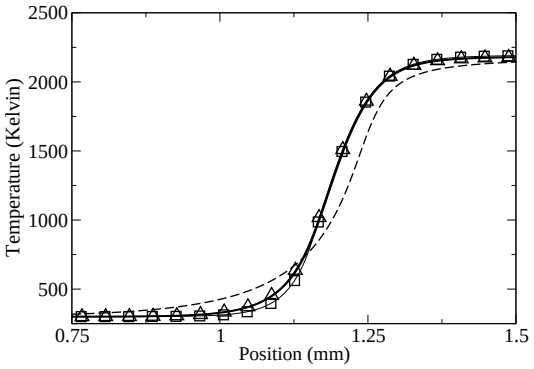

Figure 3: Filtered temperature profiles $\widetilde{T}(x)$, $\Delta/\delta_{fl} = 3$. Bold-line: Reference Eq. (10). Triangle: Eq. (15). Square: Eq. (17) with $\mathcal{F}(x)$ from Eq. (16). Dash-line: Fixed value $\mathcal{F} = 3$.

rate is also preserved within a few percent of accuracy. Figure 1 also shows $\overline{T}(x)$ obtained from filtering of the reference flame to illustrate the shift between $\overline{T}$ and $\widetilde{T}$, due to density variation. In this canonical one-dimensional problem, the deconvoluted signal, $\widetilde{\mathcal{L}}_{\Delta}^{-1}[\widetilde{T}](x)$ (square in Fig. 1) perfectly matches $T(x)$, the original one (line).

Figure 2 presents all the terms of Eq. (15) contributing to the temperature time derivative. As expected, the chemical source (circle in Fig. 2), which peaks at $c = 0.75$ in the non-filtered flame, thus on the burnt gas side, moves towards $\widetilde{c} = 0.5$ with moderate filtering and even on the fresh gas side for larger filter widths (Fig. 2(b)), a shift that is reinforced here by the fact that the terms have been divided by filtered density to examine the time derivative of temperature (Eq. (15)). The SGS convective term (Triangle) is positive in the fresh gas and negative in the burnt gases, leading to the so-called counter-gradient contribution in burnt gases (Bray 1996; Veynante, Trouvé, Bray, and Mantel 1997). It is seen that the SGS molecular diffusion (Dash-line) is of the same order than the SGS convective term in this filtered laminar flame and does not constitute a negligible contribution to the sum of the molecular diffusion terms (Square). The exact contribution of this term in a turbulent flame is still to be investigated in detail. Increasing the filter size decreases peak values of fluxes and sources.

Approximate deconvolution/filtering for source and corrective factor to resolved diffusive budget

In a turbulent jet flame, where curvature and strain are wrinkling the flame front, the modeling specific to one-dimensional filtered flames discussed above may not always be transposed. Instead, a less one-dimensional oriented approach can be used for unresolved fluxes, but still using the deconvolution for the burning rate and ensuring that the laminar flame speed is preserved whatever the mesh and the scalar signal.

In the thickened flame approach (Colin et al. 2000), it was demonstrated that the correct propagation speed of a flame front is secured applying an amplification (thickening) factor $\mathcal{F}$ to the diffusive budget expressed from mesh node values (*i.e.* $\overline{\rho a_T \nabla T} = \mathcal{F}\overline{\rho} a_T(\widetilde{T})\nabla\widetilde{T}$) and the same factor to reduce the source (*i.e.* $\overline{\dot{\omega}}_T = \dot{\omega}_T(\widetilde{T})/\mathcal{F}$), with $\mathcal{F} > 1$.

As discussed in (Merlin et al. 2012), the application of a corrective factor to the diffusive fluxes may be generalized to any modeled expression of the burning rate $\overline{\dot{\omega}}_T$, leading to a dynamically computed factor $\mathcal{F} = \dot{\omega}_T(\widetilde{T})/\overline{\dot{\omega}}_T$. Within the present approximate deconvolution/filtering, the factor $\mathcal{F}$ may be computed according to the explicitly filtered source term, to differ from unity only in the reaction zone:

$$\mathcal{F}(\underline{x},t) = \frac{\dot{\omega}_T(\widetilde{T}(\underline{x},t)))}{\overline{\dot{\omega}_T(\widetilde{\mathcal{L}}_\Delta^{-1}[\widetilde{T}(\underline{x},t)])}} \,. \tag{16}$$

The closed equation for $\widetilde{T}$ then simply reads:

$$\frac{\partial\widetilde{T}}{\partial t} = -\widetilde{u}\cdot\nabla\widetilde{T} + \frac{1}{\overline{\rho}}\nabla\cdot\left(\overline{\rho}\mathcal{F}a_T(\widetilde{T})\nabla\widetilde{T}\right) + \frac{\overline{\dot{\omega}_T(\widetilde{\mathcal{L}}_\Delta^{-1}[\widetilde{T}])}}{\overline{\rho}}. \tag{17}$$

Figure 3 shows the temperature distribution obtained with this last equation. With $\mathcal{F}$ computed dynamically from Eq. (16), the response is very close to exact filtering or to the solution of the full deconvolution (Eq. (15)), with only a small departure on the fresh gas side. For comparison, a solution was obtained using a fixed value of $\mathcal{F}$ and $\overline{\dot{\omega}}_T = \dot{\omega}_T(\widetilde{T})/\mathcal{F}$ (TFLES model (Colin et al. 2000)). This last option preserves the flame speed, but cannot reproduce carefully the filtered profile (Fig. 3 dash-line), which may become a limitation when applied to the simulation of intermediate species involved in more than a single-step reaction.

This preliminary test of approximate deconvolution and explicit filtering suggests that the method is robust to simulate with precision the behavior of a planar filtered flame front. However, this is only a canonical problem and the method is now applied to the filtered chemical reaction rate of a fully turbulent premixed flame, in order to fully access its prediction capabilities.

4 Turbulent jet-flame with tabulated detailed chemistry

The premixed stoichiometric turbulent methane flame F3 experimentally studied by Chen et al. (1996) is simulated (see Figs. 4 and 5). The piloted Bunsen burner nozzle diameter is D = 12 mm and the F3 case features a mean nozzle exit velocity of 30 m/s, with a level of turbulent kinetic energy of the order of 3.82 m^2/s^2. The temperature of the stoichiometric methane-air mixture is $T_b = 2248$ K and the pilot temperature is 1810 K. Laser diagnostics of the

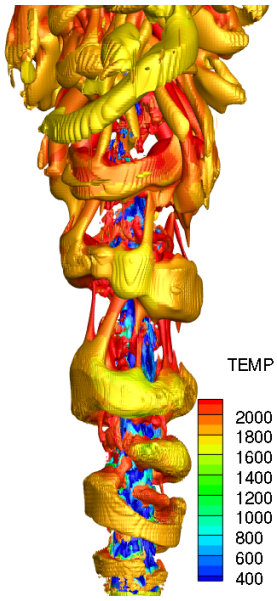

Figure 4: Contour of iso-Q criterion ($Q = 160,000$) colored by temperature.

flow field are available, they were obtained using two-component and two-point laser Doppler anenometer (LDA). Scalar fields were also experimentally reported from 2-D Rayleigh thermometry and line Raman/Rayleigh laser-induced predissociation fluorescence (LIPF)-OH techniques.

The LES mesh is composed of 306×194×194 nodes over a 16D×8D×8D computational domain, leading to a resolution varying between 170 μm and 640 μm. The simulations are performed using the SiTCom parallel flow solver already used for testing SGS combustion closures (Subramanian et al. 2010). This solver is based on an explicit Finite Volumes scheme for Cartesian grids.

The Navier-Stokes equations are in their fully compressible form together with scalars balance equations. The convective terms are computed resorting to a fourth-order centered skew-symmetric-like scheme (Ducros et al. 2000), while the diffusive terms are approximated with a fourth-order centered scheme. Time is advanced explicitly with a third order Runge-Kutta method and the 3D-NSCBC boundary conditions (Lodato et al. 2008) are used at inlet and outlet.

The SGS momentum fluxes are expressed with the Vreman model (Vreman 2004). To resolve eventual stiff gradients promoted by deconvolution, an artificial dissipation scheme was added introducing fourth order dissipative terms (Tatsumi et al. 1995).

The inlet profiles are set from the measurements to which synthetic turbulence is added (Klein et al. 2002). The total energy inlet condition accounts for the non-adiabatic character of the pilot flame.

The approximate deconvolution followed by explicit filtering may be applied to tabulated chemistry. Considering a lookup table of scalars (chemi-

cal sources, transport properties, mass fractions) $\varphi = \varphi(Y_c)$, with Y_c the control parameters of the tabulation, the filtered scalars may be written:

$$\overline{\rho}\widetilde{\varphi} = \overline{\mathcal{L}_\Delta^{-1}[\overline{\rho}]\,\varphi(\widetilde{\mathcal{L}}_\Delta^{-1}[\widetilde{Y}_c])}\,, \qquad (18)$$

where the relation (3) is used in Eq. (5).

In the present case, the chemical lookup table is build from laminar flamelets computed with the GRI-mechanism for methane-air combustion (Smith et al. 1999) and the progress variable Y_c is defined as in Godel et al. (2008).

The equations solved for the progress variable $\widetilde{Y}_c$ and total energy are similar to Eq. (17), with the chemical source obtained from the deconvolution/explicit filtering and the factor $\mathcal{F}(\underline{x},t)$ is dynamically determined by the relation (16) applied to the Y_c field.

In other words, instead of explicit filtering the diffusive term, the factor $\mathcal{F}(\underline{x},t)$ is applied to the diffusive term, whereas the source term is still obtained from deconvolution as in § 3:

$$\begin{aligned}\frac{\partial\overline{\rho}\widetilde{Y}_c}{\partial t} + \nabla\cdot\left(\overline{\rho}\widetilde{\mathbf{u}}\widetilde{Y}_c\right) &= \nabla\cdot\left(\overline{\rho}\mathcal{F}D_{Y_c}(\widetilde{Y}_c)\nabla\widetilde{Y}_c\right)\\ &+ \overline{\dot{\omega}_c(\widetilde{\mathcal{L}}_\Delta^{-1}[\widetilde{Y}_c])}\,. \qquad (19)\end{aligned}$$

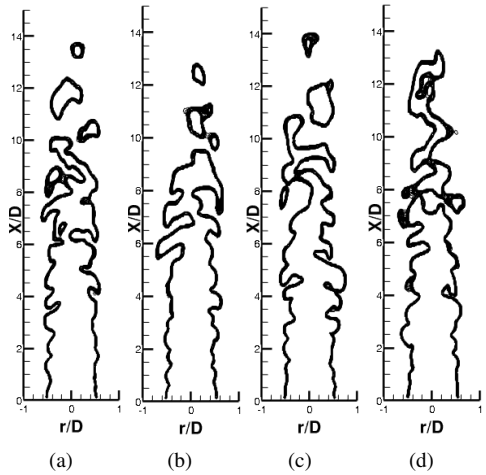

Figure 5: Time sequence of iso-$\overline{\dot{\omega}}_c$, filtered source of progress variable, $\Delta t = 1.8$ ms.

The coherent flow structure are visualized in Fig. 4 with the iso-Q criterion. The Kelvin-Helmholtz large scale vortices are rapidly connected by streamwise instabilities and alternate paring leading to spiraling vortices, these vortices feature a temperature of about 1800 K, the coflow temperature, from nozzle up to further downstream. The time sequence of iso-burning rate in Fig. 5 illustrates the quite high level of flame wrinkling, with even formation of pockets at the flame tip. The flame wrinkling may be estimated in the simulation as:

$$\Xi = \frac{\overline{|\nabla c|}}{|\nabla\overline{c}|} = \frac{\overline{|\nabla\widetilde{\mathcal{L}}_\Delta^{-1}[\widetilde{c}]|}}{\left|\nabla\overline{\widetilde{\mathcal{L}}_\Delta^{-1}[\widetilde{c}]}\right|} \qquad (20)$$

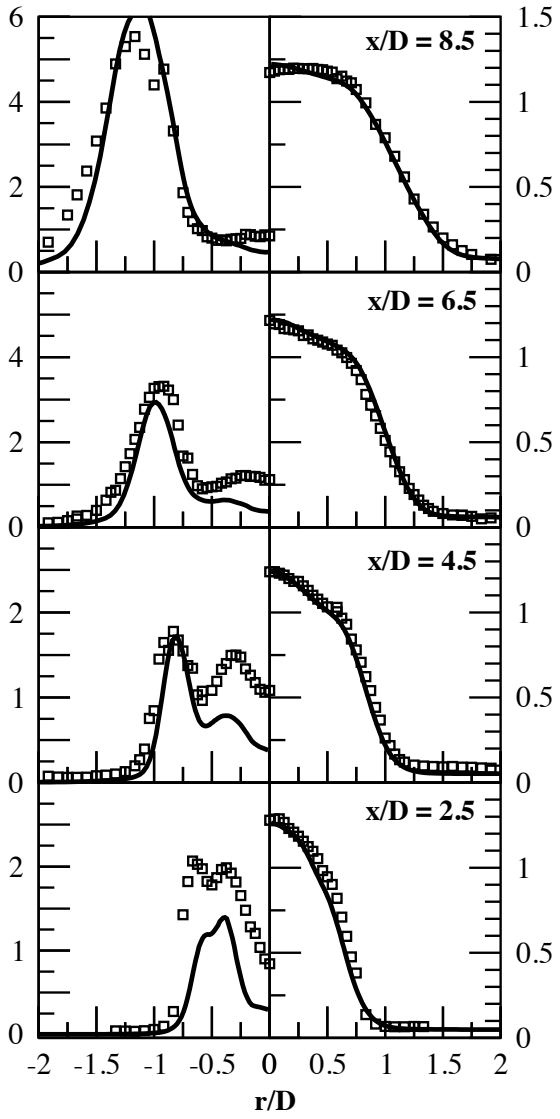

Figure 6: Symbol: measurements (Chen et al. 1996). Line: LES. (a)-Left: Turbulent kinetic energy normalized by inlet value. (a)-Right: Time averaged streamwise velocity normalized by inlet bulk velocity.

The average value of Ξ computed over the flame zone ($0.01 < c < 0.99$) at a given instant in time is $\langle\Xi\rangle = 1.1$, with a few local fluctuations up to $\Xi = 2$, thus confirming the high-level of flame resolution.

Statistics have been collected up to convergence and they are compared against experiments. The time average streamwise velocity and kinetic energy are captured (Fig. 6), with some deviation on the axis for the latter. However, the inflow forcing has not been tuned in these simulations, instead it was kept fixed to the profiles provided in the measurements at burner exit plane.

The measurements error range reported by the experimentalists is between 8% and 15% for major species concentration and up to 25% for minor species (Chen, Peters, Schneemann, Wruck, Renz,

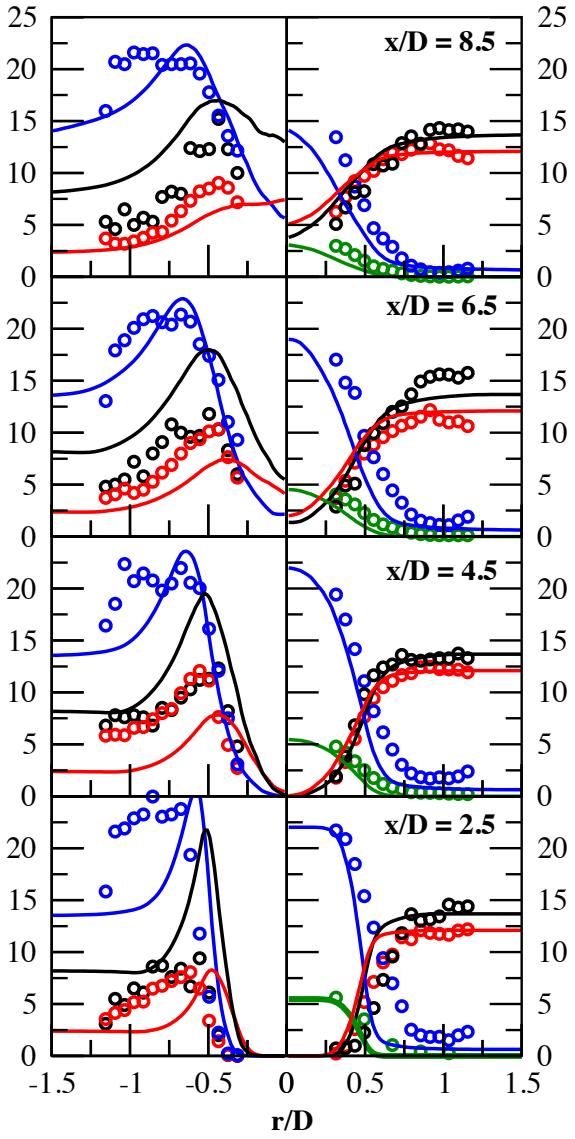

Figure 7: Mass fractions in %. Symbol: measurements. Line: LES. Left: Red: CO×10. Black: H_2×100. Blue: OH×75. Right: Blue: O_2. Green: CH_4. Red: H_2O. Black: CO_2.

and Mansour 1996). Major species O_2, CH_4, H_2O and CO_2, mainly agree with measurements within this range (Fig. 7). The prediction of minor species CO, H_2 and OH is a sensitive point using flamelet tabulation that does not include strain rate as a parameter. Results follow the experimental trend for these minor species, with the largest departure observed with H_2 (Fig. 7).

5 Summary

A novel approach is discussed for Large Eddy Simulation (LES) of premixed turbulent combustion, which is valid with high order numerics along with grid resolution providing quite resolved scalar signals. It is based on an approximate and discrete deconvolution of density weighted scalars so that unclosed terms can be estimated on the LES mesh, to be subsequently explicitly filtered.

The method is first tested for a one-dimensional laminar filtered flame, using a single-step Arrhenius reaction rate. Two options are proposed and compared for the fluxes, a full deconvolution, or, the application of a dynamically computed corrective factor to the diffusive flux computed from the resolved scalar signal.

Then, the approximate deconvolution/filtering of the burning rate is applied to three-dimensional LES of a turbulent Bunsen flame (Chen et al. 1996), using tabulated detailed chemistry. Most of the statistical properties of both velocities and scalars are reproduced. The modeling procedure is free from any adjustable parameter, aside from numerical interpolation and/or high-order damping of scalar gradients, and can be readily applied to any chemical scheme, opening new perspective for turbulent combustion modeling, specifically to address intermediate species and pollution with LES.

Acknowledgment

This work was granted access to the HPC resources of IDRIS under the allocation 2013-020152 made by GENCI (Grand Equipement National de Calcul Intensif).

References

Boudier, G., L. Y. M. Gicquel, and T. J. Poinsot (2008). Effects of mesh resolution on large eddy simulation of reacting flows in complex geometry combustors. *Combust. Flame 155*(1-2), 196–214.

Bray, K. N. C. (1996). The challenge of turbulent combustion. *Proc. Combust. Inst. 26*, 1–26.

Chen, Y.-C., N. Peters, G. A. Schneemann, N. Wruck, U. Renz, and M. S. Mansour (1996). The detailed flame structure of highly stretched turbulent premixed methane-air flames. *Combust. Flame 107*(3), 223–244.

Colin, O., F. Ducros, D. Veynante, and T. Poinsot (2000). A thickened flame model for large eddy simulations of turbulent premixed combustion. *Physics of Fluids 12*(7), 1843–1863.

Domingo, P., L. Vervisch, S. Payet, and R. Hauguel (2005). Dns of a premixed turbulent v-flame and les of a ducted-flame using a fsd-pdf subgrid scale closure with fpi tabulated chemistry. *Combust. Flame 143*(4), 566–586.

Domingo, P., L. Vervisch, and D. Veynante (2008). Large-eddy simulation of a lifted methane-

air jet flame in a vitiated coflow. *Combust. Flame 152*(3), 415–432.

Ducros, F., F. Laporte, T. Soulères, V. Guinot, P. Moinat, and B. Caruelle (2000). High-order fluxes for conservative skew-symmetric-like schemes in structured meshes: application to compressible flows. *J. Comput. Phys. 161*, 114–139.

Fiorina, B., R. Vicquelin, P. Auzillon, N. Darabiha, O. Gicquel, and D. Veynante (2010). A filtered tabulated chemistry model for les of premixed combustion. *Combust. Flame 157*, 465–475.

Godel, G., P. Domingo, and L. Vervisch (2008). Tabulation of nox chemistry for large-eddy simulation of non-premixed turbulent flames. *Proc. Combust. Inst. 32*, 1555–1561.

Hawkes, E. R. and R. S. Cant (2001). Implications of a flame surface density approach to large eddy simulation of premixed turbulent combustion. *Combust. Flame 126*(3), 1617–1629.

Katopodes, F., R. L. Street, and J. H. Ferziger (2000). Subfilter-scale scalar transport for large eddy simulation. In *14th Symposium on Boundary Layers an Turbulence*, pp. 472–475. American Meteorologic Society.

Kim, W.-W., S. Menon, and H. C. Mongia (1999). Large-eddy simulation of a gas turbine combustor flow. *Combust. Sci. and Tech. 143*, 25–62.

Klein, M., A. Sadiki, and J. Janicka (2002). A digital filter based generation of inflow data for spatially developing direct numerical or large eddy simulations. *J. Comp. Physics 186*(2), 652–665.

Kuenne, G., F. Seffrin, F. Fuest, T. Stahler, A. Ketelheun, D. Geyer, J. Janicka, and A. Dreizler (2012). Experimental and numerical analysis of a lean premixed stratified burner using 1d raman/rayleigh scattering and large eddy simulation. *Combust. Flame 159*(8), 2669–2689.

Lecocq, G., S. Richard, O. Colin, and L. Vervisch (2011). Hybrid presumed pdf and flame surface density approach for large-eddy simulation of premixed turbulent combustion, part 1: Formalism and simulations of a quasi-steady burner. *Combust. Flame 158*(6), 1201–1214.

Lele, S. K. (1992). Compact finite difference schemes with spectral like resolution. *J. Comput. Phys. 103*, 16–42.

Lodato, G., P. Domingo, and L. Vervisch (2008). Three-dimensional boundary conditions for direct and large-eddy simulation of compressible viscous flows. *J. Comput. Phys 227*(10), 5105–5143.

Merlin, C., P. Domingo, and L. Vervisch (2012). Large eddy simulation of a turbulent flame in a trapped vortex combustor (tvc) - a flamelet presumed-pdf closure preserving laminar flame speed. *C. R. Mecanique 340*(11-12), 917–932.

Moureau, V., P. Domingo, and L. Vervisch (2011). From large-eddy simulation to direct numerical simulation of a lean premixed swirl flame: Filtered laminar flame-pdf modeling. *Combust. Flame 158*(7), 1340–1357.

Moureau, V., B. Fiorina, and H. Pitsch (2009). A level set formulation for premixed combustion les considering the turbulent flame structure. *Comb. and Flame 156*, 801–812.

Nambully, S., P. Domingo, V. Moureau, and L. Vervisch (2014a). A filtered-laminar-flame pdf sub-grid scale closure for les of premixed turbulent flames. part I: Formalism and application to a bluff-body burner with differential diffusion. *Combust. Flame 161*(7), 1756–1774.

Nambully, S., P. Domingo, V. Moureau, and L. Vervisch (2014b). A filtered-laminar-flame pdf sub-grid scale closure for les of premixed turbulent flames: Part II: Application to a stratified bluff-body burner. *Combust. Flame 161*(7), 1775–1791.

Peters, N. (2000). *Turbulent Combustion*. Cambridge University Press.

Smith, G. P., D. M. Golden, M. Frenklach, N. W. Moriarty, B. Eiteneer, M. Goldenberg, C. T. Bowman, R. K. Hanson, S. Song, W. C. Gardiner, V. V. Lissianski, and Z. Qin (1999). Technical report. http://www.me.berkeley.edu/grimech/.

Subramanian, V., P. Domingo, and L. Vervisch (2010). Large-Eddy Simulation of forced ignition of an annular bluff-body burner. *Combust. Flame 157*(3), 579–601.

Tatsumi, S., L. Martinelli, and A. Jameson (1995). Flux-limited schemes for the compressible navier-stokes equations. *AIAA Journal 33*(2).

Veynante, D., A. Trouvé, K. Bray, and T. Mantel (1997). Gradient and counter-gradient scalar transport in turbulent premixed flames. *J. Fluid Mech. 332*, 263–293.

Vreman, A. W. (2004). An eddy-viscosity subgrid-scale model for turbulent shear flow: Algebraic theory and applications. *Phys. Fluids. 16*(10).